balt5/z1g-jcn/z1g-jcn/z1g00610/z1g2451-10a | wasifk | S=4 | 10/21/10 | 14:05 | 4/Color Figure(s): F1,F7 | Art: WNP200355 | Input-bs

Aberrant Neuronal Avalanches in Cortical Tissue Removed From Juvenile Epilepsy Patients

Jon P. Hobbs,† Jodi L. Smith,‡ and John M. Beggs*†*

Abstract: Some forms of epilepsy may arise as a result of pathologic interactions among neurons. Many forms of collective activity have been identified, including waves, spirals, oscillations, synchrony, and neuronal avalanches. All these emergent activity patterns have been hypothesized to show pathologic signatures associated with epilepsy. Here, the authors used 60-channel multielectrode arrays to record neuronal avalanches in cortical tissue removed from juvenile epilepsy patients. For comparison, they also recorded activity in rat cortical slices. The authors found that some human tissue removed from epilepsy patients exhibited prolonged periods of hyperactivity not seen in rat slices. In addition, they found a positive correlation between the branching parameter, a measure of network gain, and firing rate in human slices during periods of hyperactivity. This relationship was not present in rat slices. The authors suggest that this positive correlation between the branching parameter and the firing rate is part of a positive feedback loop and may contribute to some forms of epilepsy. These results also indicate that neuronal avalanches are abnormally regulated in slices removed from pediatric epilepsy patients.

Key Words: Epilepsy, Synchrony, Multiple electrode array, Neural network, Cortex, *In vitro*, Avalanche.

(*J Clin Neurophysiol* 2010;27: 000–000)

Epilepsy is a complex disorder, and any comprehensive attempt to understand it will likely consist of approaches at many scales (Wong et al., 1986), from studies of ion channel dysfunction (Dingeldine et al., 1999) to anatomic malformations (Sisodiya, 2000). However, regardless of cause, all forms of epilepsy are characterized by excessive activity in large numbers of neurons (Dwyer et al., 2010; Nita et al., 2006). This excessive activity could be produced by hyperexcited neurons acting independently or it could involve abnormal interactions among many neurons.

To explore the hypothesis that some forms of epilepsy are caused, at least in part, by aberrant interactions among neurons, it is important to record activity from many neurons simultaneously. Potentially abnormal interactions then could be identified as patterns of collective activity in epileptic tissue that were not present in nonepileptic tissue. Many investigators have used multielectrode arrays (Jimbo and Kawana, 1992), calcium imaging (Tashiro et al., 2002), or voltage-sensitive dyes (Blasdel and Salama, 1986) to record activity from multiple sites, and several important types of collective activity have been implicated in epilepsy. These include waves (Tsau et al., 1999), synchrony (Wilke et al., 2009), asynchrony (Schiff et al., 1994), high-frequency oscillations (Traub et al., 2009), and spirals (Netoff et al., 2004; van Drongelen et al., 2005).

Recently, a new form of collective activity, called neuronal avalanches, has been identified in neocortex (Beggs and Plenz, 2003). These avalanches are characterized by cascades of neural activity whose sizes can be approximated by a power law distribution, such as avalanches in sand pile models (Bak, 1996; Bak et al., 1988). Because neuronal avalanches were originally reported in cortical slice cultures and acute cortical slices *in vitro*, they have been identified in rats and primates *in vivo* (Gireesh and Plenz, 2008; Petermann et al., 2009). In addition, several studies have linked them to activity in human subjects, suggesting that they are a very general phenomenon (Poil et al., 2008; also see Touboul and Destexhe, 2010). Why would so many networks seem to show these neuronal avalanches? Modeling work indicates that neuronal avalanches may be optimal for information transmission, information storage, and extending dynamic range (Beggs, 2008; Beggs and Plenz, 2003, 2004; Buice and Cowan, 2009; Chen et al., 2010; Haldeman and Beggs, 2005; Kinouchi and Copelli, 2006; Shew et al., 2009; Thiagaragian and Plenz, 2009; van Drongelen et al., 2005).

Computational models also have explored the potential relationship between neuronal avalanches and epilepsy (Hsu and Beggs, 2006; Hsu et al., 2007, 2008). Briefly, this work suggests that healthy brains regulate their activity so that they operate near a critical point, where they produce neuronal avalanches. At this critical point, activity in one neuron is on average followed by activity in one other neuron (Beggs and Plenz, 2003; Chen et al., 2010; Chialvo, 2006; Haldeman and Beggs, 2005; Pajevic and Plenz, 2009). This relationship can be quantified by the branching parameter, which is the ratio of the number of "descendant" neurons to the number of "ancestor" neurons. A branching parameter of one is indicative of the critical point. Although this critical point may seem trivial to attain, it is not. Pharmacological agents that reduce excitatory or inhibitory synaptic transmission move networks away from the critical point (Beggs and Plenz, 2003; Shew et al., 2009). In addition, when network activity is randomly shuffled, it no longer follows a power law distribution characteristic of avalanches (Beggs, 2008). Thus, operating at the critical point depends on the appropriate balance of inhibition and excitation and results in structured activity that is far from random. From this perspective, epileptic activity would occur when regulatory mechanisms failed and the network entered a super critical regimen. There, the branching parameter would exceed one and activity in one neuron would, on average, lead to activity in more than one neuron, amplifying activity excessively and possibly leading to seizures.

In this article, we examined activity in local cortical networks within the framework of neuronal avalanches. We used 60-channel multielectrode arrays to record local field potentials (LFPs) in slices removed from pediatric epilepsy patients. For comparison, we also recorded LFPs in slices of rat cortex. Slices of human cortex had periods of pronounced hyperexcitability. Our analysis showed that during these periods, there was a significant positive correlation between the branching parameter and the firing rate, suggesting a positive feedback loop. This relationship was not present in activity observed in

From the *Indiana University Program in Neural Science; †Indiana University Department of Physics, Bloomington; and ‡Indiana University School of Medicine, Indianapolis, Indiana, U.S.A.

Supported by Pence foundation (to J.L.S.) and Neural Science Teaching fellowship (to J.P.H).

Address correspondence and reprint requests to Jon P. Hobbs; e-mail: jonxhobbs@gmail.com.

ISSN: 0736-0258/10/2706-0001

<zjs;Original Article> • <zjss;Original Article> • <zdoi;10.1097/WNP.0b013e3181fdf8d3>

balt5/z1g-jcn/z1g-jcn/z1g00610/z1g2451-10a | wasifk | S=4 | 10/21/10 | 14:05 | 4/Color Figure(s): F1,F7 | Art: WNP200355 | Input-bs

rat cortex. These results indicate that neuronal avalanches are abnormally regulated in slices removed from pediatric epilepsy patients.

METHODS

Data Used in This Study

This study comprised data from human and rat cortical tissue. Cortical tissue was harvested from patients (Fig. 1A) who were already undergoing resective surgery for the treatment of intractable epilepsy and who gave written informed consent to donate tissue for this Institutional Review Board-approved study (IRB 0612, Indiana University School of Medicine, Indianapolis, IN).

The cortical tissue was obtained from the most active epileptogenic area of the patient's seizure focus as identified by intraoperative electrocorticography (Fig. 1B). Only tissue from the area that was to be resected as part of the surgical treatment of the patient's intractable seizures was used in this study. A 2 × 2 mm piece of cortex within the seizure focus was removed immediately after the intraoperative electrocorticography; removal took <30 seconds. The tissue was then transported to the laboratory using a custom-made transport device (Fig. 1C). Typically, transporting the tissue from the operating room to the adjacent laboratory for slicing took 3 minutes.

The tissue analyzed in this study was obtained from 31 pediatric patients during the period of June 2006 to May 2009. Because this study focused on collective interactions, only tissue with 45 or more active electrodes was included. Furthermore, to ensure adequate sampling for statistical significance, we included only recordings with robust activity lasting ≥45 minutes. Tissue from only 6 of 31 patients that we studied met these criteria. All six of the included patients had seizures localized to the temporal lobe (Table 1). In all patients, the seizures were localized to an area of cerebral cortex containing tumor surrounded by an area of epilep-

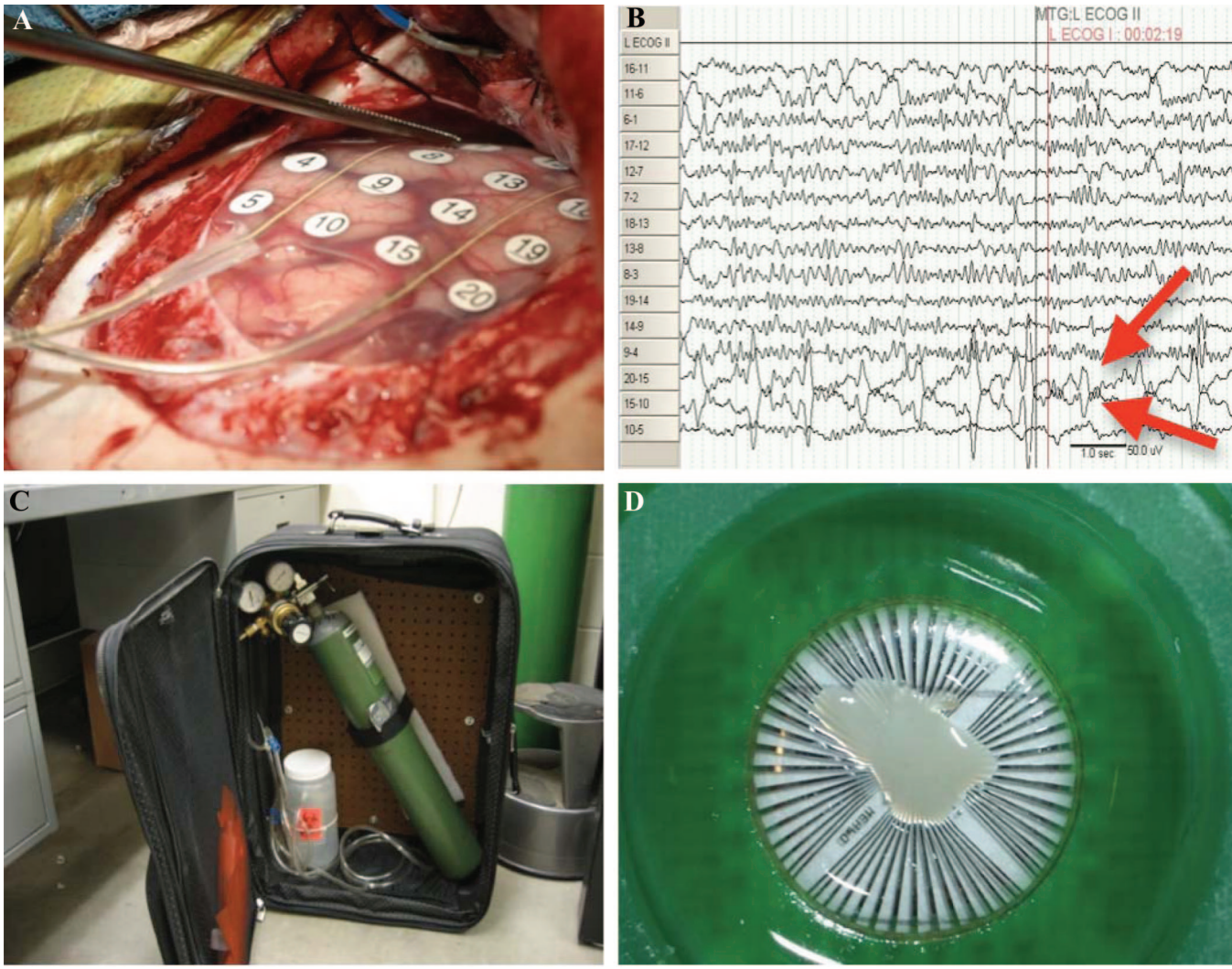

FIGURE 1. Procedures for tissue collection and preparation. Exposed human temporal lobe cortex with surface electrode array (**A**). *In vivo* electrocorticography trace (**B**) from surface electrodes is read by a physician to determine the region of the putative epileptic foci. In this trace, the tissue under electrodes 20 to 15 and 15 to 20 (gray arrows) was identified for removal. Transport chamber (**C**) used to transfer the tissue to the laboratory after it had been sectioned into thin slices in the adjacent operating room. An image of the sliced tissue (**D**) on the electrode array (electrode leads appear as four metallic pie-shaped bundles converging to the center).

togenic cortex as identified by preoperative video EEG and intraoperative electrocorticography.

For comparison, rat tissue was collected from Sprague-Dawley strain rats 18 to 35 days old approved for use in this study. The tissue produced LFPs for many hours on >45 electrodes. Coronal sections of rat somatosensory cortex were used (N = 6).

Tissue Preparation and Recording

Human tissue was prepared in accordance with IRB 0612 (Indiana University School of Medicine, Indianapolis, IN). Approval from guardians or parents of patients was obtained before surgery. All patients voluntarily elected to be in the study. Putative epileptic foci were identified by a trained physician before resection of the tissue in all cases. Cerebral vasculature was left intact as the tissue was resected. As white matter was visible in the tissue block, it was possible to orient the block so that coronal sections would be cut. The dorsal section was easily identifiable, as coagulation occurs quickly at the dorsal surface while the tissue is cut out intraoperatively. Tissue blocks from rats were prepared as previously reported (Tang et al., 2008). All procedures were approved by the Indiana University Animal Care and Use Committee. Sprague-Dawley rats 14 to 35 days old (Harlan, Indianapolis, IN) were deeply anesthetized with halothane and then decapitated. Tissue blocks from both humans and rats were immediately placed for 3 minutes in ice-cold artificial cerebrospinal fluid (ACSF) containing (in mM) sucrose 125, KCl 3, $NaH_2PO_4 \cdot H_2O$ 1.25, $NaHCO_3$ 26, $MgSO_4 \cdot 7H_2O$ 2, $CaCl_2 \cdot 2H_2O$ 2, and D-glucose 10 and saturated with 95% O_2/5%CO_2. The block of tissue was then sliced into coronal sections with a thickness of 250 μm using a tissue slicer (Vibratome 3000 series, Myneurolab).

TABLE 1. Human Tissue Characteristics

Patients	Gender	Age (Years)	Pathology
H1	M	14.9	DNET, WHO* grade 1
H2	F	10.4	Ganglioglioma, WHO* grade 2
H3	M	10	Stroke
H4	F	6.3	Ganglioglioma, WHO* grade 1
H5	F	12	Ganglioglioma, WHO* grade 1
H6	F	8	Ganglioglioma, WHO* grade 1

*World Health Organization rating of tumor grades increasing in severity from 1. DNET, dysembryoplastic neuroepithelial tumor.

After cutting, slices were bathed for ~1 hour at room temperature in ACSF with the same ingredients as listed above but with 125 mM NaCl substituted for 125 mM sucrose to restore Na^+ and allow cells to fire action potentials again. In preparation for recording, slices were adhered to microelectrode arrays with a solution of 0.1% polyethyleneimine that had been previously applied and let to dry for 2 hours (Wirth and Luscher, 2004). We attempted to place the tissue so that neocortical layers I to V covered the array. Slices were maintained thermostatically at 37°C and were perfused at 1.0 mL/min first with normal ACSF for 1 hour to see whether the tissue was spontaneously active. If spontaneous activity did not develop after 1 hour, the tissue was bathed in excitable ACSF solution containing 5 mM KCl and 0 mM Mg^{2+}. These external ionic concentrations are known to produce robust LFP activity in cortical brain slices (Schiff et al., 1994; Wu et al., 1999).

Electrode Arrays

Recordings were performed on microelectrode arrays purchased from Multichannel Systems (Reutlingen, Germany). Each array had 60 electrodes, and each electrode was 30 μm in diameter and 30 μm in height. Electrodes were arranged in a square grid with 200-μm spacing between electrodes (Fig. 2A). F2

Local Field Potential Detection

Extracellular activity from slices was recorded in the same manner as previously reported (Beggs and Plenz, 2003, 2004; Tang et al., 2008). Activity was sampled from all 60 electrodes (Fig. 2B) at 1 kHz and amplified before being stored to disk for offline analysis. LFPs that showed sharp negative peaks (Fig. 2B) below a threshold set at 3SD of the signal were marked, and the time of the maximum excursion was recorded as the time of that LFP (Fig. 2C). Time points were binned at 4 milliseconds resolution, as this was previously shown to match the average time between successive LFP events across electrodes (Beggs and Plenz, 2003).

Characterizing Multielectrode Activity

In characterizing network activity, we closely followed the methods first described in the study by Beggs and Plenz (2003, 2004) and illustrated in Fig. 3. The configuration of active electrodes during one time step is called a frame. F3

An avalanche is a sequence of consecutively active frames that is preceded by a blank frame and terminated by a blank frame. The length of an avalanche is given by the total number of active frames, and the size of an avalanche is given by the total number of electrodes activated during the avalanche.

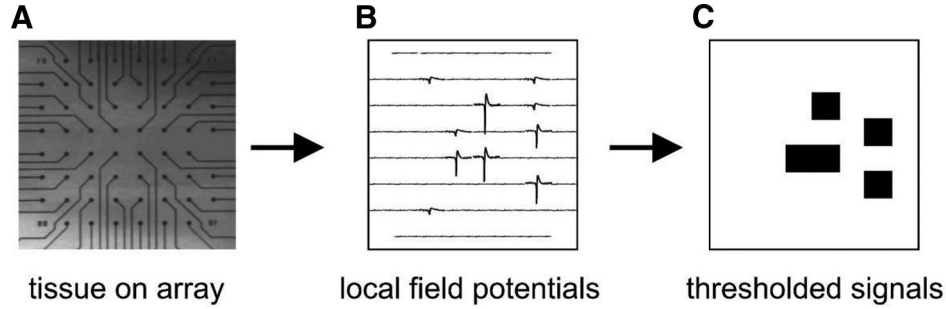

FIGURE 2. Electrode array and data representation. Rat cortical tissue on the 60-channel microelectrode array (**A**). An image from beneath the tissue is super imposed on top showing the electrodes that appear as small black circles at the ends of lines. Interelectrode distance is 200 μm and electrode diameter is 30 μm. Local field potential (LFP) signals on electrodes at one time step (**B**). Note that LFPs can vary in amplitude. A threshold of 3SD is applied to the recording. Suprathreshold LFPs are represented by small black squares (**C**).

balt5/z1g-jcn/z1g-jcn/z1g00610/z1g2451-10a | wasifk | S=4 | 10/21/10 | 14:05 | 4/Color Figure(s): F1,F7 | Art: WNP200355 | Input-bs

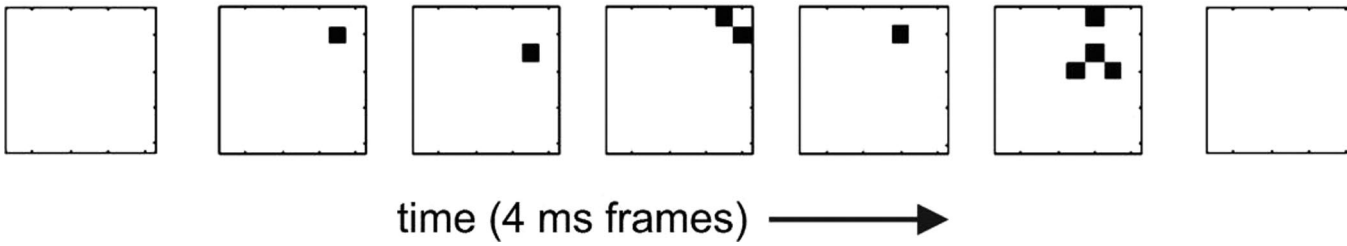

FIGURE 3. Example of an avalanche. Seven frames are shown, where each frame represents activity on the electrode array during one 4-millisecond time step. Suprathreshold activity at electrodes is shown by small black squares. An avalanche is a series of consecutively active frames that is preceded by and terminated by blank frames. Avalanche length is given by the number of active frames, whereas avalanche size is given by the total number of active electrodes. The avalanche shown here has a length of 5 and a size of 9.

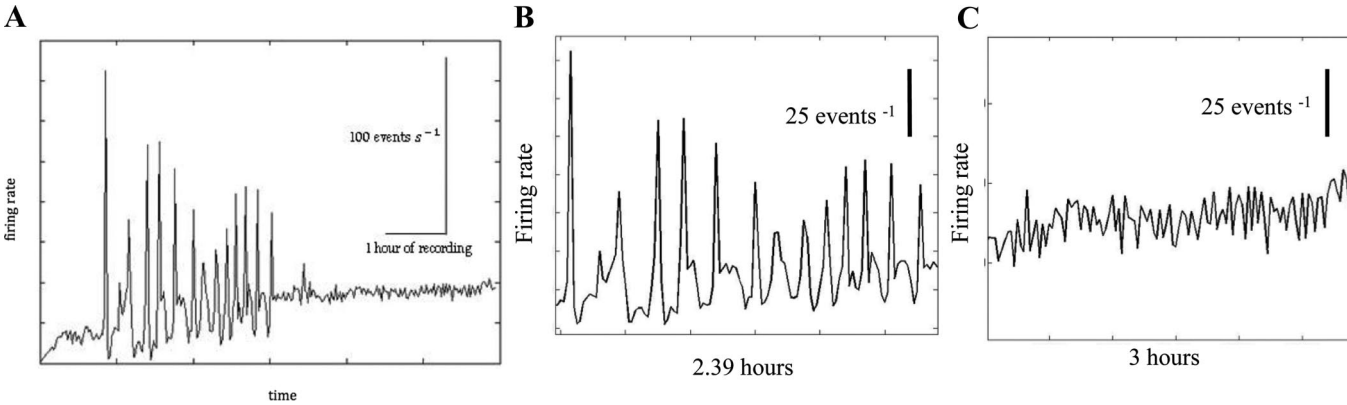

FIGURE 4. Examples of elevated and nonelevated firing periods. Firing rate plotted as a function of time (**A**) for one representative human slice. Scale bar indicates 100 events s^{-1} and 1 hour of recording. This tissue exhibited a long period of elevated firing 1 hour into the recording, and the activity was sustained for nearly 3 hours until it resumed a "normal" firing rate again for several more hours. Human tissue often exhibited these two distinct regimes. In our analysis, we separated elevated activity (**B**) from "normal" activity (**C**).

Measuring the Branching Parameter

The branching parameter, symbolized by σ, is the average number of descendant electrodes produced by a single ancestor electrode. By ancestor electrode, we mean an electrode on the array that experienced a suprathreshold LFP signal at a given time step. By descendant electrode, we mean an electrode on the array that experienced a suprathreshold LFP signal one time step after the activity of the ancestor electrode. The branching parameter is straightforward to approximate from experimental data and can be obtained by taking the ratio:

$$\sigma = \left\langle \frac{N_{2:L}}{N_{1:(L-1)}} \right\rangle,$$

where L is the length of each avalanche, $N_{2:L}$ is the total number of electrodes activated in frames 2 to L, $N_{1:(L-1)}$ is the total number of electrodes activated in frames 1 to $L-1$, and the angled brackets indicate averaging over all avalanches. From this definition, it is clear that the branching parameter is a measure of collective excitability in the network. Intuitively, when $\sigma < 1$, activity is damped and will quickly die out. When $\sigma = 1$, the network is in the critical state, and long chains of neural activity can occur without unstable expansion. When $\sigma > 1$, activity is amplified every time step, eventually leading to excessive network activity.

RESULTS

Spontaneous Activity in Human Slices

When bathed in normal ACSF, human slices usually displayed little or no spontaneous activity. On one occasion, we observed activity on 45 or more electrodes that lasted for 30 minutes in normal ACSF; however, this activity abruptly ended.

For all other human slices, despite being removed from putative epileptogenic areas, spontaneous activity was always limited to not >15 electrodes in normal ACSF. When perfused with ACSF containing elevated K^+ and reduced Mg^{2+}, almost all these slices displayed some spontaneous activity.

Local Field Potentials in Human and in Rat Tissue

Local field potential activity from human and rat slices was similar to that reported previously (Beggs and Plenz, 2003, 2004; Tang et al., 2008) and consisted of quiescent periods punctuated by network bursts. Local field potentials that crossed threshold appeared as negative voltage peaks ~20 milliseconds wide, indicative of a population spike (Fig. 2B). Such sharp negative LFPs are thought to be produced by a group of neurons in the vicinity of the electrode firing nearly synchronous action potentials (Johnston and Wu, 1995). Data were binned at 4 milliseconds, as this was the average time between successive activation of two electrodes within a network burst when the inter electrode spacing was 200 μm, as reported previously (Beggs and Plenz, 2003).

balt5/z1g-jcn/z1g-jcn/z1g00610/z1g2451-10a | wasifk | S=4 | 10/21/10 | 14:05 | 4/Color Figure(s): F1,F7 | Art: WNP200355 | Input-bs

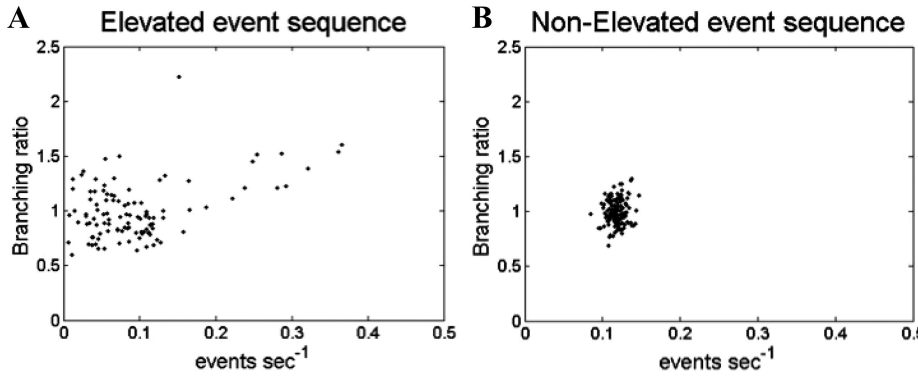

FIGURE 5. Positive feedback loop in human tissue. During elevated activity (**A**), there was a positive and significant correlation between the firing rate and the branching parameter, $P < 0.05$. During normal activity (**B**), there was no significant correlation between the firing rate and the branching parameter. Data are from the same representative example human slice shown in Fig. 4. The positive correlation between the firing rate and the branching parameter only occurred in human tissue (N = 4) and only occurred during intervals of elevated activity.

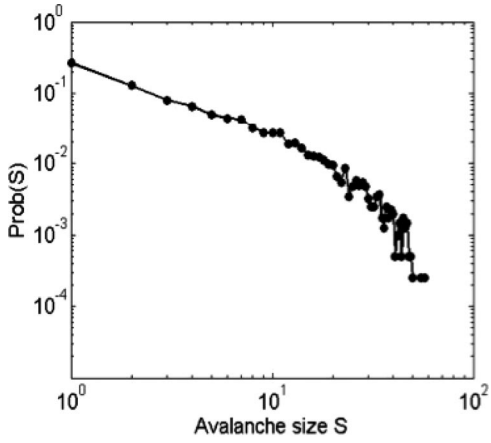

FIGURE 6. Representative event size distribution from rat. The probability of an event size as a function of the observed avalanche size in log-log scale. The size distribution of avalanches can be approximated by a −3/2 power law in rats.

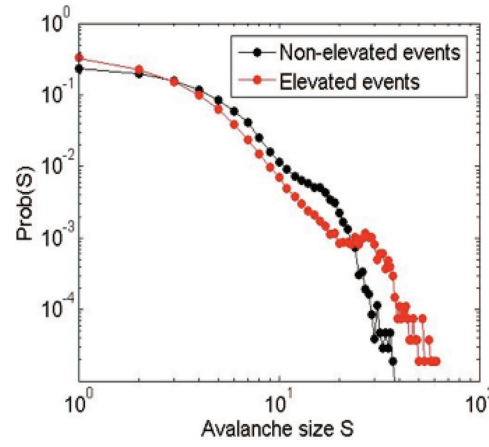

FIGURE 7. Event size distribution from human. The elevated and nonelevated event sequence avalanche distributions plotted together. The elevated (red/gray) sequence has a hump around event size 30 electrodes. Nonelevated sequence (black) does not exhibit this hump.

Periods of Hyperactivity

We measured network firing rate by counting the number of array electrodes driven over threshold per second. In data obtained from rat cortical slices, firing rate was on average 0.558 ± 0.28 Hz (mean ± SD) and varied relatively little over the duration of the recording. Data obtained from slices removed from epilepsy patients had an average firing rate of 0.87 ± 0.64 Hz. Notably, four of six human datasets showed periods of elevated firing rate (Fig. 4A), where the momentary firing rate (averaged over a 45-second interval) exceeded the mean firing rate by 2.5SD on more than two occasions during the recording session. Typically, human slices oscillated between periods of elevated firing and normal firing for ≥1 hour (Fig. 4B). In contrast, rat slices never exhibited these pronounced swings in firing rate (Fig. 5).

Event Size Distributions

We commonly observed LFPs that exceeded the threshold on multiple electrodes in the same time bin. We also observed cascades of consecutively active time bins (Fig. 2). After cascades were recorded over 45 minutes or more, it was possible to plot their size distribution. For data collected from rats, this size distribution had a very long tail that approached a power law (Fig. 6). Because this distribution was not expected by chance (Beggs, 2008), but was similar to that produced by computational models of sand pile avalanches (Bak, 1996), we previously named these events "neuronal avalanches" (Beggs and Plenz, 2003).

The cascade size distribution from human tissue typically looked different from that produced by rat tissue as shown in Fig. 7. Human tissue produced downwardly curving plots. These plots looked slightly different, depending on whether the data were taken from inside (red/gray) or outside (black) the elevated period.

Branching Parameter and Firing Rate

In the rat data, the average branching parameter was 0.74 ± 0.26. We examined the relationship between the branching parameter and the firing rate in each rat cortical slice network and found that these two variables were never significantly correlated. In the human data, the average branching parameter over the entire duration of each recording was 0.42 ± 0.171. These branching parameter values are significantly different, $P = 0.042$ (*t*-test), alpha = 0.05.

balt5/z1g-jcn/z1g-jcn/z1g00610/z1g2451-10a | wasifk | S=4 | 10/21/10 | 14:05 | 4/Color Figure(s): F1,F7 | Art: WNP200355 | Input-bs

TABLE 2. Summary of Data Collected From Rats and Humans

File Name	Elevated Segment (Seconds)	Branching Value	Correlation Coefficient	*P*	Firing Rate (Hz)	Normal Segment (Seconds)	Branching Value	Correlation Coefficient	*P*	Firing Rate (Hz)
Humans										
H1	All	0.6121	0.6269	0.0000	0.3811	None	None	None		
H2	None					All	0.5529	−0.4549	0.0008	0.43
H3						All	0	−0.0871	0.3862	0.05
H4	All	0.29	0.47	0.0001	0.27	None	None			
H5	1,800–7,200	0.8661	0.4295	0.0000	0.5565	7,200–13,365	0.9332	0.1548	0.0622	0.6592
H6	0–4,050	0.26	0.6935	0.0000	0.8756	4,050–12,915	0.0005	0.00	0.00	0.0689
Rats										
R1	None						0.84	0.198	0.2194	0.771
R2	None					All	0.633	−0.137	0.2965	0.432
R3	None					All	1.1163	0.126	0.336	0.745
R4	None					All	0.928	0.0632	0.6314	0.524
R5	None					All	0.5572	0.23	0.0782	0.926
R6	None						0.4036	−0.0364	0.7822	0.819

Statistical characterization of elevated and nonelevated periods from humans and rats show significant swings in activity in humans (N = 4).

TABLE 3. Recording Length and Suprathreshold Activity

File Name	Recording Length (Hours)	Suprathreshold
Humans		
H1	1.69	20
H2	0.86	0
H3	1.69	0
H4	1	2
H5	0.86	2
H6	5	11
Rats		
R1	1	1
R2	1	0
R3	1	0
R4	1	0
R5	1	0
R6	1	1

We did not find a significant relationship between the number of elevated periods and the cumulative suprathreshold counts.

Interestingly, we found that there was a significant positive correlation between the branching parameter and the firing rate during periods of hyperactivity (N = 4, Table 2). This significant correlation was not present during nonhyperactive periods, and it was not present in the rat data (Table 3).

Branching Parameter Significantly Lower During Hyperactivity

The fact that the branching parameter was positively correlated to the firing rate led us to go back and calculate the average branching parameter separately during periods of hyperactivity and during periods of lower firing rate. Surprisingly, we found that the branching parameter was significantly lower during periods of hyperactivity than during nonhyperactive periods. The *t*-test was significant, $P = 0.0442$.

DISCUSSION

Main Finding

The main finding of this work is that cortical tissue removed from pediatric epilepsy patients produces aberrant neuronal avalanches. Four specific features of this activity appear different from what is found in rat cortical tissue: periods of hyperactivity, lack of a clear power law in avalanche size distributions, positive correlation between firing rate and branching parameter, and significantly lower branching parameter during hyperactive periods.

Validity

Although these results are statistically significant, caution must be exercised in extrapolating these findings to activity in humans *in vivo*. Of primary concern is that we were only able to examine slices that were removed from the intact brain. The process of making slices necessarily severs long-range connections, producing alterations of cortical circuitry. In addition, our results are based on only six human samples. It is extremely difficult to obtain such tissue slices and even more difficult to get them to produce viable activity over periods of several hours. More samples are clearly needed to establish the generality of these findings.

Finally, it would have been more scientifically appropriate to compare human cortical tissue removed from epilepsy patients with cortical tissue removed from nonepileptic patients or at least from areas of cortex that did not show epileptiform activity. Although such healthy tissue is occasionally removed from neurosurgical patients to allow access to a tumor, this tissue is very rare and we could not obtain any for this study. Instead, we used rat cortical tissue for comparison. Across-species comparisons of cortical activity should be viewed with caution.

Implications

In computational models, an increase in the branching parameter, a measure of network "gain," causes the network firing rate also to increase (Haldeman and Beggs, 2005). This is because each suprathreshold event would trigger, on average, more events than before.

Thus, it has been hypothesized that the branching parameter itself is regulated in cortical networks so that it decreases when firing rate increases. Indeed, very generic computational models

require this negative feedback arrangement for network stability (Hsu and Beggs, 2006; Hsu et al., 2007). These models also suggest that firing rate homeostasis, by itself, is not sufficient to prevent runaway network excitation. The branching parameter must also be regulated (Hsu et al., 2007). The experimental findings here indicate local cortical networks with a positive correlation between the branching parameter and firing rate also show extended periods of hyperactivity.

This suggests that these slices show hyperactivity precisely because they fail to regulate the branching parameter. The idea that this positive feedback loop would contribute to epilepsy is natural, intuitively appealing, and consistent with our model and the data.

How the branching parameter is regulated, and how these putative regulatory mechanisms could fail, will be important topics for future research.

Yet, another result from this study is still puzzling. Why does the branching parameter decrease during periods of hyperactivity? This result is not new and is consistent with earlier work done in rat tissue. Beggs and Plenz (2003) showed that the power law distribution of avalanche sizes can be disrupted by the application of picrotoxin. Picrotoxin is a γ-aminobutyric acid-A antagonist and, interestingly, causes the branching parameter to decrease in rat cortical slice networks (Plenz, 2005). One of the novel contributions of this study is to show that the branching parameter decreases in human tissue from epilepsy patients during periods of hyperactivity. Both these results are counterintuitive, because one would expect that increased network activity would be accompanied by an increase in network gain. How can we account for this?

We can think of two possible explanations. First, during periods of excessive activity, there is often also increased synchrony (Worrell et al., 2004). This could cause many electrodes to have suprathreshold activity in the same time bin, rather than across several time bins. If this was the case, then many avalanches would have ancestors in the same time bin, leaving few or no descendants in subsequent time bins. Such a situation would lower the branching parameter. We examined this in our limited dataset of six human slices and found that sometimes this appears to be what is happening. However, we need more data to evaluate this hypothesis.

Second, it is known that the branching parameter can be underestimated in some situations (Priesemann et al., 2009). In particular, if the distance between electrodes is increased in an avalanche model with local connectivity, the observed branching parameter will decrease, even if the data are sampled at longer time bins to account for longer propagation times between electrodes. Although we did not change the electrode distance in our experiments, it is possible that the dynamics of some avalanches changed during periods of hyperactivity, causing them to propagate in a more compact manner or more rapidly. If this is the case, then the relationship between electrode distance and the average distance between successive events in an avalanche would change. This could cause the observed branching parameter to decrease. Again, we have anecdotal evidence for this in some cases, but we will need more human data before we can clearly state whether this is consistently occurring.

ACKNOWLEDGMENT

The authors thank all the patients and their parents who contributed cortical tissue to this research and the Pence Foundation for their commitment to finding a cure for epilepsy.

REFERENCES

AQ: 10

Bak P. *How Nature Works: The Science of Self-Organized Criticality*. New York, NY: Copernicus; 1996.

Bak P, Tang C, Wiesenfeld. Self-organized criticality. *Phys Rev A.* 1988;38:364–374.

Beggs JM. The criticality hypothesis: how local cortical networks might optimize information processing. *Philos Transact A Math Phys Eng Sci*. 2008;366:329–343.

Beggs JM, Plenz D. Neuronal avalanches in neocortical circuits. *J Neurosci*. 2003;23:11167–11177.

Beggs JM, Plenz D. Neuronal avalanches are diverse and precise activity patterns that are stable for many hours in cortical slice cultures. *J Neurosci*. 2004;24:5216–5229.

Blasdel GG, Salama G. Voltage-sensitive dyes reveal a modular organization in monkey striate cortex. *Nature*. 1986;321:579–585.

Buice MA, Cowan JD. Statistical mechanics of the neocortex. *Prog Biophys Mol Biol*. 2009;99:53–86.

Chen W, Hobbs JP, Tang A, Beggs JM. A few strong connections: optimizing information retention in neuronal avalanches. *BMC Neurosci.* 2010;11:3.

Chialvo DR. Are our senses critical? *Nat Phys*. 2006;2:301–302.

Dingledine R, Borges K, Bowie D, Traynelis SF. The glutamate receptor ion channels. *Pharmacol Rev.* 1999;51:7–62.

Dwyer J, Lee H, Martell A, et al. Oscillation in a network model of neocortex. *Neurocomputing*. 2010;73:1051–1056.

Gireesh ED, Plenz D. Neuronal avalanches organize as nested theta- and beta/gamma-oscillations during development of cortical layer 2/3. *Proc Natl Acad Sci USA*. 2008;105:7576–7581.

Haldeman C, Beggs JM. Critical branching captures activity in living neural networks and maximizes the number of metastable states. *Phys Rev Lett*. 2005;94:058101.

Hsu D, Beggs JM. Neuronal avalanches and criticality: a dynamical model for homeostasis. *Neurocomputing.* 2006;69:1134–1136.

Hsu D, Chen W, Hsu M, Beggs JM. An open hypothesis: is epilepsy learned, and can it be unlearned? *Epilepsy Behav*. 2008;13:511–522.

Hsu D, Tang A, Hsu M, Beggs JM. Simple spontaneously active Hebbian learning model: homeostasis of activity and connectivity, and consequences for learning and epileptogenesis. *Phys Rev E Stat Nonlin Soft Matter Phys*. 2007;76(4 pt 1):041909.

Jimbo Y, Kawana A. Electrical stimulation and recording from cultured neurons using a planar electrode array. *Bioelectrochem Bioenerg*. 1992;29:193–204.

Johnston D, Wu SM. *Foundations of Cellular Neurophysiology*. Cambridge, MA: MIT Press; 1995.

Kinouchi O, Copelli M. Optimal dynamic range of excitable networks at criticality. *Nature Physics.* 2006;2:348–351.

Netoff TI, Clewley R, Arno S, et al. Epilepsy in small-world networks. *J Neurosci*. 2004;24:8075–8083.

Nita DA, Cissé Y, Timofeev I, Steriade M. Increased propensity to seizures after chronic cortical deafferentation in vivo. *J Neurophysiol*. 2006;95:902–913.

Pajevic S, Plenz D. Efficient network reconstruction from dynamical cascades identifies small-world topology of neuronal avalanches. *PLoS Comput Biol.* 2009;5:e1000271.

Petermann T, Thiagarajana TC, Lebedevb MA, et al. Spontaneous cortical activity in awake monkeys composed of neuronal avalanches. *Proc Natl Acad Sci USA*. 2009;106:15921–15926.

Plenz D. Comment on "Critical branching captures activity in living neural networks and maximizes the number of metastable states." *Phys Rev Lett*. 2005;95:219801; author reply 219802.

Plenz D, Thiagarajan TC. The organizing principles of neuronal avalanches: cell assemblies in the cortex? *Trends Neurosci.* 2007;30:101–110.

Poil SS, Van Ooyen A, Linkenkaer-Hansen K. Avalanche dynamics of human brain oscillations: relation to critical branching processes and temporal correlations. *Human Brain Mapping.* 2008;29:770–777.

Priesemann V, Munk MH, Wibral M. Subsampling effects in neuronal avalanche distributions recorded in vivo. *BMC Neurosci*. 2009;10:40.

Schiff SJ, Jerger K, Duong DH, et al. Controlling chaos in the brain. *Nature*. 1994;370:615–620.

Shew WL, Yang H, Petermann T, et al. Neuronal avalanches imply maximum dynamic range in cortical networks at criticality. *J Neurosci*. 2009;29:15595–15600.

Sisodiya SM. Surgery for malformations of cortical development causing epilepsy. *Brain.* 2000;123:1075–1091.

Tang A, Jackson D, Hobbs J, et al. A maximum entropy model applied to spatial and temporal correlations from cortical networks in vitro. *J Neurosci*. 2008;28:505–518.

Tashiro A, Goldberg J, Yuste R. Calcium oscillations in neocortical astrocytes under epileptiform conditions. *J Neurobiol.* 2002;50:45–55.

Touboul J, Destexhe A. Can power-law scaling and neuronal avalanches arise from stochastic dynamics? *PLoS One*. 2010;5:e8982.

Traub RD. Fast oscillations and epilepsy. *Epilepsy Curr.* 2003;3:77–79.

Tsau Y, Guan L, Wu JY. Epileptiform activity can be initiated in various neocortical layers: an optical imaging study. *J Neurophysiol*. 1999;82:1965–1673.

van Drongelen W, Lee HC, Hereld M, et al. Emergent epileptiform activity in neural networks with weak excitatory synapses. *IEEE Trans Neural Syst Rehabil Eng*. 2005;13:236–241.

Wilke C, Worrell GA, He B. Analysis of epileptogenic network properties during ictal activity. *Conf Proc IEEE Eng Med Biol Soc*. 2009;2009: 2220–2223.

Wirth C, Luscher HR. Spatiotemporal evolution of excitation and inhibition in the rat barrel cortex investigated with multi-electrode arrays. *J Neurophysiol*. 2004;91:1635–1647.

Wong RKS, Traub RD, Miles R. Cellular basis of neuronal synchrony in epilepsy. *Adv Neurol*. 1986;44.

Worrell GA, Parish L, Cranstoun SD, et al. High-frequency oscillations and seizure generation in neocortical epilepsy. *Brain*. 2004;127(pt 7):1496–1506.

Wu JY, Guan L, Tsau Y. Propagating activation during oscillations and evoked responses in neocortical slices. *J Neurosci*. 1999;19:5005–5015.